This is an author-created, un-copyedited version of the article G. N. Phung and U. Arz, "Parasitic Probe Effects in Measurements of Coplanar Waveguides with Narrow Ground Width,"2020 IEEE 24th Workshop on Signal and Power Integrity (SPI), Cologne, Germany, 2020, pp. 1-4.

The definitive publisher-authenticated version is available online at: https://doi.org/10.1109/SPI48784.2020.9218166

Parasitic Probe Effects in Measurements of Coplanar Waveguides with Narrow Ground Width

Gia Ngoc Phung
Physikalisch-Technische Bundesanstalt (PTB)
Bundesallee 100,
38116 Braunschweig
gia.phung@ptb.de

Uwe Arz
Physikalisch-Technische Bundesanstalt (PTB)
Bundesallee 100,
38116 Braunschweig
uwe.arz@ptb.de

***Abstract*—On-wafer measurements contain a large variety of parasitic effects degrading the accuracy of multiline Thru-Reflect Line (mTRL) calibration. These effects are caused by internal and external disturbances such as probe effects, multimode propagation, crosstalk between adjacent structures and radiation effects. While a lot of investigations have been performed for the most common coplanar waveguides (CPW) with nominal ground width, CPW with too narrow ground width have not been investigated thoroughly. This paper demonstrates how the probe effects deteriorate the mTRL-calibrated S-parameters for CPW structures with narrow ground width.**

Keywords— calibration, coplanar waveguides, multiline Thru-Reflect Line (mTRL), probes.

I. Introduction

On-wafer measurements are of fundamental importance for the characterization of components and devices in high-speed and microwave applications ranging from wireless communications, automotive radar and medical sensing. However, for on-wafer measurements, a lot of challenges need to be addressed. On-wafer probing with ground-signal-ground (GSG) probes itself contains a lot of parasitic effects which are not to be underestimated. On the one hand, these effects can be initiated by the impact of neighborhood, measurement environment, multimode propagation and the measurement instrumentation itself. On the other hand, they are caused by the actual characteristics of the device under test (DUT), mainly radiation and dispersion effects. In recent years, a major effort has been undertaken to investigate and to clarify the sources of these parasitic effects. In [1] the influence of microwave probes on calibrated on-wafer measurements is demonstrated for the coplanar waveguides (CPW) and thinfilm microstriplines (TFMSL) up to W-Band. Similar investigations have been performed in [2,3] for the extended frequency range up to 330 GHz. In [4,5] the occurrence of parasitic substrate modes was discussed. The latter investigation suggested measures to mitigate the propagation of substrate modes.

In [6-8] the impact of radiation losses has been thoroughly explained. It has been detected that the influence of the CPW ground width is one of the main causes for radiation losses and dispersion effects [7]. The impact of wide CPW ground width has been clarified thoroughly in [8]. A recommendation has been proposed to keep the total CPW w_{tot} which represents two times the ground-to-ground spacing plus double the ground width smaller than the formula given in [7,8]. A priori the ultimate maximum applicable CPW ground width which allows decent CPW characteristics is therefore defined. So, one would assume that reducing the CPW ground width would be the best choice to avoid any radiation and dispersion effects. However, this might not be true and gives rise to the question how the CPW characteristics would change when the CPW ground width is reduced to a minimum. Starting from a measurement example, this paper demonstrates how the *S*-parameters of the coplanar structures with reduced CPW ground width change in interaction with probe effects. For a better understanding, 3 D full-wave electromagnetic simulations in CST [9] are performed*.

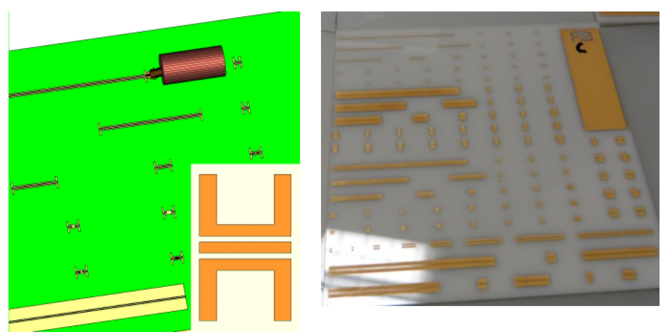

(a) (b)

Fig. 1. a.) Electromagnetic model of a complete wafer with probe excitation in CST [9]; b.) Investigated wafer with three different calibration sets.

Fig. 1 shows the investigated wafer which has been used in [10,11] and designed for the investigation of parasitic effects. The wafer consists of three different calibration sets with common CPW parameters of CPW signal width of $w = 50$ µm, a gap of $s = 25$ µm and varied CPW ground widths of $w_g = 50$, 270 and 650 µm. The calibration set consists of a short as reflect standard, a 400 µm long CPW line as thru and eight additional lines with lengths between 500 and 20400 µm. All

*) We use brand names only to better specify the experimental conditions. PTB does not endorse commercial products. Other products may work as well or better.

the measurements are performed with GGB* probes with a 100 µm pitch.

In the simulation, a detailed probe model [1,10] is applied. Both the simulated and measured data are processed with the multiline Thru-Reflect-Line (mTRL) calibration algorithm [12] to reveal the true performance of the DUT.

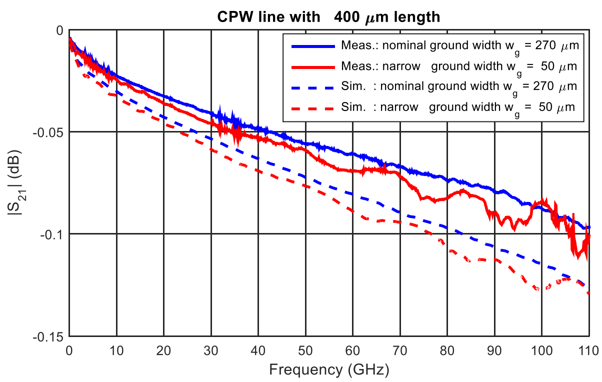

Fig. 2. Measurement and simulation result of a CPW line with length of $l = 400$ µm.

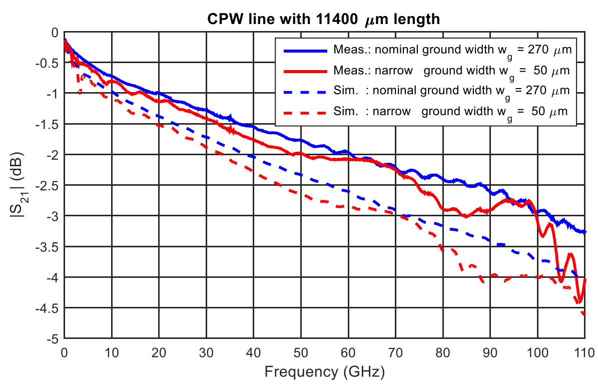

Fig. 3. Measurement and simulation result of a CPW line with length of $l = 11400$ µm.

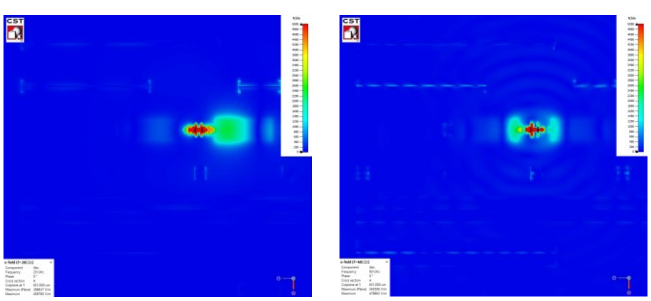

(a) (b)

Fig. 4. Simulation of the electric field magnitude of the complete wafer with probes for the CPW line with length of $l = 400$ µm and narrow CPW ground width of $w_g = 50$ µm at a.) $f = 20$ GHz and b.) $f = 60$ GHz.

Figs. 2 and 3 show the simulated and measured calibrated S_{21} - parameter of a 400 µm and 11400 µm CPW line. What is varied, is the CPW ground width w_g with 270 µm and 50 µm (with a special pad configuration). At first sight, one can state that the simulation results show a reasonably good agreement with the measurements. The deviations can be explained by the insufficient knowledge of material parameters in the simulation. What is more important to note is that ripples for the narrow CPW case occur in both CPW lines whereas the nominal CPW case exhibits a smoother curve behavior. This indicates that reducing the CPW ground width itself adds additional parasitic effects. The field plots in Fig. 4 reveal that neither the crosstalk behavior between adjacent structures nor probe coupling with neighboring structures is the main cause responsible for the ripples occurring in the simulation and measurement results. Furthermore, the field plots do not imply that multimode or substrate mode propagation would be contributing to this ripple effect. Therefore, a possible cause might be the interaction of parasitic fields from the probe contact with the pads which will be studied in the next section.

II. Systematic Study

A. *Influence of CPW Ground Width*

The first step of the study is to simplify the investigation by using a single DUT which is only excited by the probes. Therefore, the interference of neighboring structures and multimode propagation are excluded.

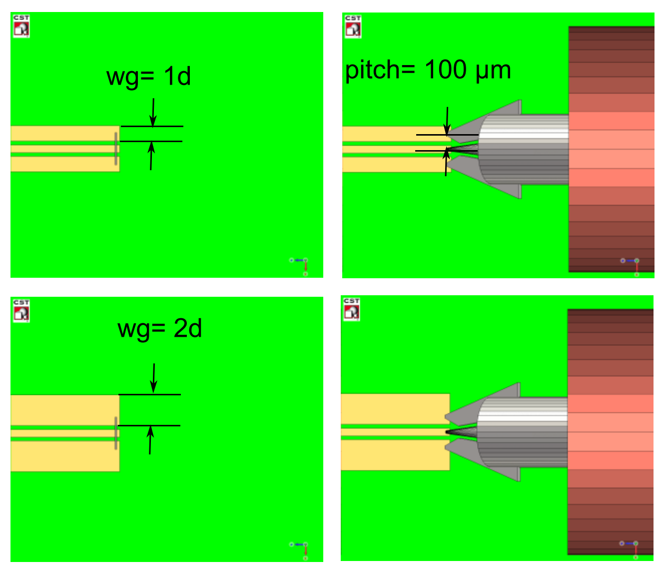

(a) (b)

Fig. 5. Simulation model with different excitation and varying CPW ground width $w_g = 1d$ and $2d$. a.) bridge model; b.) probe model.

In order to clarify the ripple effect, a bridge model shown in Fig. 5a is used as a reference. This simplified model makes use of a conducting bridge between the ground planes of the CPW structure. A lumped element is placed in the center of the signal conductor to excite the structure. This model has been used in several investigations [1,5,10] to represent the most ideal, least parasitics excitation of CPW structures.

Two parameters are examined; the CPW ground width w_g is varied between $1d$, $1.5d$ and $2d$ (whereas d represents the ground-to-ground spacing – in this case 100 µm) with both excitation modi, the bridge model in Fig. 5a and probe model in Fig. 5b.

Fig. 6 clearly demonstrates that the simulation results applying the bridge model do not differ much for the three different CPW ground widths $w_g = 1d$, $1.5d$ and $2d$. This indicates that the ripple effect is not mainly caused by the CPW characteristics itself. The simulation results of the CPWs excited by the probe model on the other hand show divergent results for the three different cases. The probe simulation with $w_g = 1d$ shows an emphasized ripple effect whereas the ripples in the curve behavior disappear with larger w_g. The case with $w_g = 2d$ for example exhibits a smooth curve behavior. The smaller the ground width w_g, the stronger the ripples. This implies that the causes of the ripple effect originate from the interaction of probe effects at the transition of the probe needles to the coplanar pads. Thus, to clarify this unexpected behavior, electric fields at the probe contact are illustrated for the two different cases of $w_g = 1d$ and $2d$.

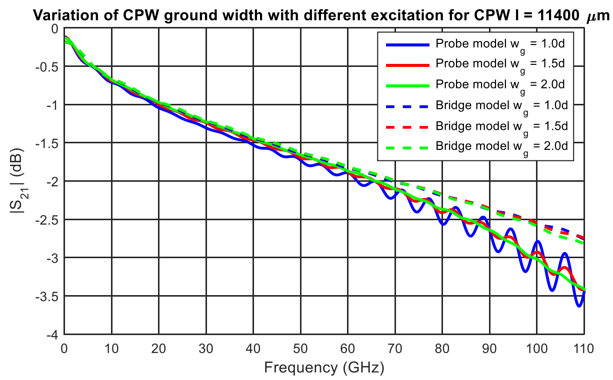

Fig. 6. Raw simulation results of a 11400 µm CPW line with different ground widths w_g excited by probe model in comparison with the bridge model.

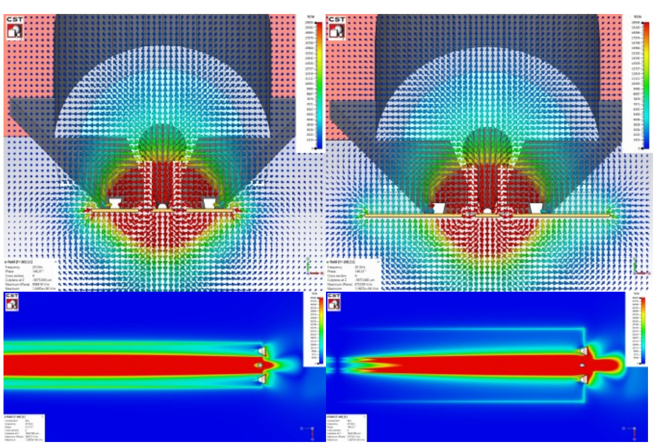

(a) (b)

Fig. 7. Electric field vector (top: at probe contact) and electric field distribution (bottom: at 1 µm above the metalization) at f =20 GHz for CPW (length l = 11400 µm) with varied ground width a.) $w_g = 1d$ and b.) $w_g = 2d$.

Fig. 7 shows a comparison of the electric fields for $w_g = 1d$ and $2d$. Obviously, the probe transition at the coplanar pads is not ideal. If the CPW ground width is too narrow (Fig. 7a), there are pronounced field discontinuities at the edge of the probe contact. Stray fields at the edge of the CPW can be clearly observed. The distraction of the fields at the coplanar edge prevents the excitation of a pure CPW mode and, additionally the parasitic stray fields are propagating along the length of the CPW line (Fig. 7a bottom). The conventional pure CPW mode is therefore distorted. A wider CPW ground of minimum $w_g = 2d$ reduces the field discontinuities at the edge of CPW (see Fig. 7b top). Stray fields at the edge of the coplanar pads are mitigated (see Fig. 7b bottom) and therefore the ripples in the transmission curve also vanish with larger CPW ground width.

So far, we have used standard probe dimensions with a probe pitch of 100 µm. To really assign the causes of the ripple effects to the field discontinuities of probe transition at the coplanar pads, one needs to verify the investigation by varying the probe pitches to see whether this behavior changes with different probe pitches.

B. Influence of Probe Pitch

In the following, we use the case of $w_g = 2d$ where the simulation results of the standard pitch of 100 µm already show smooth curve behavior and enlarge the probe pitch in 50 µm steps from 100 till 200 µm.

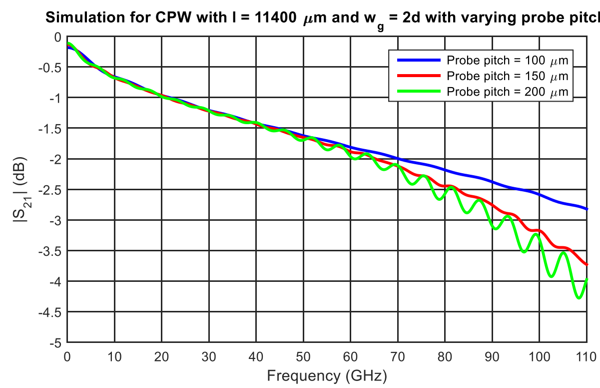

Fig. 8. Raw simulation results of a 11400 µm CPW line with $w_g = 2d$ excited by probe model of different probe pitches.

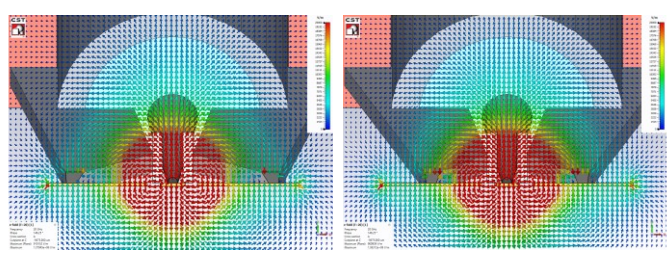

(a) (b)

Fig. 9. Electric field vector at probe contact at f = 20 GHz for probe pitch of a.) 200 µm and b.) 150 µm.

Interestingly, Fig. 8 reveals that the ripples reoccur again in the results of the CPW excited by probe with larger probe pitch of 200 µm. This clarifies that the field discontinuities at the probe transition are responsible for the ripple effects detected in the measurement and simulation results. The field plots in Fig. 9 support this statement. The field discontinuities at the edge of the probe transition contribute mainly to parasitics especially when the probe needles are laterally positioned next to the edge of the CPW.

III. Summary

Summarizing the above results, one can state that the field discontinuities at the probe transition in CPW with narrow ground width are the main causes for the ripple effects detected in the measurements. On the one hand, the CPW ground width needs to be chosen small enough to avoid the propagation of higher order modes [7,8]. On the other hand, a too narrow CPW ground width adds additional parasitic effects degrading the accuracy of the calibrated measurements due to the field discontinuities of the probe transition to the coplanar pads. Thus, the choice of CPW ground width in combination with probe effects needs to be properly considered in MMIC design.

Acknowledgment

The authors acknowledge support by the European Metrology Programme for Innovation and Research (EMPIR) Project 14IND02 “Microwave measurements for planar circuits and components”. Furthermore, this work was supported in part by 18SIB09 “Traceability for electrical measurements at millimetre-wave and terahertz frequencies for communications and electronics technologies”. Both projects (14IND02 and 18SIB09) have received funding from the EMPIR programme co-financed by the Participating States and from the European Union's Horizon 2020 research and innovation programme.

References

[1] G. N. Phung *et al.*, "Influence of Microwave Probes on Calibrated On-Wafer Measurements," in *IEEE Transactions on Microwave Theory and Techniques*, vol. 67, no. 5, pp. 1892–1900, May 2019.

[2] D. Müller *et al.*, "Electromagnetic field simulation of MMICs including RF probe tips," *2017 47th European Microwave Conference (EuMC)*, Nuremberg, 2017, pp. 900–903.

[3] D. Müller, F. Boes, A. Tessmann, A. Leuther, T. Zwick and I. Kallfass, "Crosstalk analysis and correction in on-wafer measurements at WR-3 band frequencies," *2018 11th German Microwave Conference (GeMiC)*, Freiburg, 2018, pp. 160–163.

[4] E. M. Godshalk, "Surface Wave Phenomenon in Wafer Probing Environments," *40th ARFTG Conference Digest*, Orlando, FL, USA, 1992, pp. 10–19.

[5] G. N. Phung, F. J. Schmückle, R. Doerner, W. Heinrich, T. Probst and U. Arz, "Impact of Substrate Modes on mTRL-Calibrated CPW Measurements in G Band," *2018 48th European Microwave Conference (EuMC)*, Madrid, 2018, pp. 194–197.

[6] M. Y. Frankel, S. Gupta, J. A. Valdmanis, and G. A. Mourou, “Terahertz attenuation and dispersion characteristics of coplanar transmission lines,” *IEEE Trans. Microw. Theory Techn.*, vol. 39, no. 6, pp. 910–916, Jun. 1991.

[7] F. Schnieder, T. Tischler and W. Heinrich, "Modeling dispersion and radiation characteristics of conductor-backed CPW with finite ground width," in *IEEE Transactions on Microwave Theory and Techniques*, vol. 51, no. 1, pp. 137–143, Jan. 2003.

[8] M. Spirito, *et al*., Guidelines for the design of calibration substrates, including the suppression of parasitic modes for frequencies up to and including 325 GHz : EMPIR 14IND02 – PlanarCal, 2018. DOI: https://doi.org/10.7795/530.20190424A

[9] CST Microwave Studio Suite®, https://www.cst.com/ 2-1900, Feb. 2020.

[10] G. N. Phung, F. J. Schmückle, R. Doerner, W. Heinrich, T. Probst and U. Arz, "Effects Degrading Accuracy of CPW mTRL Calibration at W Band," *2018 IEEE/MTT-S International Microwave Symposium - IMS*, Philadelphia, PA, 2018, pp. 1296–1299.

[11] T. Probst, R. Doerner, M. Ohlrogge, R. Lozar and U. Arz, "110 GHz on- wafer measurement comparison on alumina substrate," *2017 90th ARFTG Microwave Measurement Symposium (ARFTG)*, Boulder, CO, 2017, pp. 1–4.

[12] R. B. Marks, “A multiline method of network analyzer calibration,” *IEEE Trans. Microw. Theory Techn.*, vol. 39, no. 7, pp. 1205–1215, Jul. 1991.